MALAYSIAN JOURNAL OF MICROSCOPY

Journal homepage: https://malaysianjournalofmicroscopy.org

RESEARCH ARTICLE

THE EFFECTS OF OVEROXIDATION ON THE MORPHOLOGICAL AND ELECTRICAL PROPERTIES OF POLYANILINE (PANI) BASED SOLID POLYMER ELECTROLYTE (SPE)

Nur Najiha Maliaman[1], Saiful Arifin Shafiee[2], Muhammad Zharfan Mohd Halizan[3], Awatif Hassim[1], Siti Nur Amira Shaffee[4], Muhammad Faiz Aizamddin[4], Mohamad Arif Kasri[1,2], Mohd Muzamir Mahat[1*]

[1]Faculty of Applied Sciences, Universiti Teknologi MARA, 40450 Shah Alam, Selangor, Malaysia.

[2]Department of Chemistry, Kulliyyah of Science, International Islamic University Malaysia, Jalan Sultan Ahmad Shah, 25200 Kuantan, Pahang, Malaysia.

[3]Faculty of Applied Sciences, Universiti Teknologi MARA, 02600 Arau, Perlis, Malaysia.

[4]Group Research and Technology, PETRONAS Research Sdn. Bhd., Bandar Baru Bangi 43000 Selangor, Malaysia.

Abstract. Overoxidation in lithium-ion batteries (LIBs) can occur when a solid polymer electrolyte (SPE) undergoes extreme oxidation, forming undesirable functional groups like carbonyl and hydroxyl. This work examines the effects of overoxidation on polyaniline (PANI)-based SPEs, focusing on morphological, electrical, and structural changes. SPE films composed of PANI, polyethylene oxide (PEO), polyvinylidene fluoride (PVDF), and lithium bis(trifluoromethanesulfonyl)imide (LiTFSI) were prepared with varying PANI concentrations (1 wt.%, 3 wt.%, and 5 wt.%) and subjected to overoxidation via cyclic voltammetry (CV). Fourier-transform infrared spectroscopy (FTIR) was used to characterize the structural changes, while electrochemical impedance spectroscopy (EIS) assessed electrical conductivity. The highest initial conductivity (1.8×10^{-5} S/cm) was observed in the composite with 1 wt.% PANI, decreasing to 1.79×10^{-6} S/cm after overoxidation. Composites with 3 wt.% and 5 wt.%. PANI exhibited lower initial conductivities of 1.41×10^{-6} S/cm and 1.25×10^{-6} S/cm, respectively, which further dropped to 4.17×10^{-7} S/cm and 1.79×10^{-7} S/cm post-overoxidation. Field-emission scanning electron microscopy (FESEM) revealed that the interpenetrating polymer network (IPN) structures present before treatment were disrupted after overoxidation. FTIR confirmed the formation of hydroxyl and carbonyl species, which correlate with reduced conductivity and degradation of the SPE material. These findings illustrate the detrimental effects of overoxidation on PANI-based SPEs, impacting their structural integrity, morphology, and electrical performance. This has significant implications for LIB efficiency and highlights the importance of mitigating overoxidation in SPEs.

Keywords: Polyaniline, overoxidation, interpenetrating network, conducting polymer, solid polymer electrolyte.

Article Info

Received 14 August 2024
Accepted 5 October 2025
Published 4 December 2025

***Corresponding author: mmuzamir@uitm.edu.my**
Copyright Malaysian Journal of Microscopy (2025). All rights reserved.
ISSN: 1823-7010, eISSN: 2600-7444

1. INTRODUCTION

In 1975, Wright found that combining alkaline metal ions with polyethylene oxide (PEO) yielded ionic conductivity of 1×10^{-7} S/cm at room temperature, sparking research to enhance SPE conductivity under ambient conditions [1]. Solid polymer electrolytes (SPEs) attract interest in lithium-ion batteries due to their low cost, good mechanics, safety, electrode compatibility, and easy processing. Li-ion transport occurs through segmental motion in the amorphous regions of the polymer host [2]. SPEs are formed by dissolving Li salts into polar polymer hosts such as PEO or PPO, then casting films via solution casting or hot pressing. Polyether-lithium salt complexes typically show ionic conductivity of 10^{-8}-10^{-7} S/cm at room temperature due to high crystallinity [3]. High crystallinity hinders ionic transport in SPEs, as ion movement primarily occurs in the amorphous phase and is facilitated by polymer segmental mobility [3]. Enhancing the amorphous region of SPEs improves ionic conductivity by suppressing polymer crystallization, thereby increasing chain flexibility and mobility. This can be achieved by incorporating an interpenetrating polymer network (IPN) [1]. An IPN is a polymer formed by interlacing two or more networks at the molecular scale, shown to enhance SPE conductivity and mechanical strength by reducing crystallinity [4]. These properties make IPNs useful in LIBs, supercapacitors, and solar cells. For instance, a supercapacitor electrode was developed by embedding poly(3,4-ethylenedioxythiophene) (PEDOT), a conductive polymer, into an ionically conducting polymer matrix [5]. The study aimed to develop semi-IPNs (sIPNs) of PEDOT with PEO and compare them to bare PEDOT. The sIPN electrode showed higher specific capacitance, as PEO stores ions around PEDOT, reducing ion diffusion distance and enabling charge storage. This concept supports the development of interpenetrating materials with intrinsically conducting polymers (ICPs), driving research on their use in LIB electrodes and separators [3].

ICPs are π-conjugated polymers that conduct electricity through alternating single and double bonds in the backbone, including structures like polyacetylene and monomers such as pyrrole, aniline, phenylene, and thiophene. Overoxidation can occur during synthesis when oxidants like ammonium persulfate (APS), used to polymerize polypyrrole (PPy) and polyaniline (PANI), are exposed to gaseous media such as air [6]. Overoxidation in ICPs can also occur under high positive electrode potentials or harsh oxidizing conditions, leading to major changes in their properties and molecular structure [6]. Overoxidation from high voltage occurs faster than air oxidation, as rapid electron transfer accelerates degradation, while air oxidation is slower and temperature dependent. This process disrupts the π-conjugated system in ICPs, altering their chemical and physical properties, reducing conductivity, and introducing defects that impair device performance. Controlling oxidation is therefore crucial, as excessive degradation disables redox activity in SPE films and diminishes LIB performance. PANI, however, remains a promising SPE material due to its electrical, sensing, redox, antioxidant, anticorrosive, and magnetic properties [7]. Though PANI experiences electrochemical overoxidation at high anodic potentials, leading to significant degradation and the formation of quinone-like compounds such as hydroquinone/benzoquinone (HQ/BQ) [8]. ICP overoxidation occurs when ICP is charged above a specific threshold. Cyclic voltammetry (CV) can be used to study PANI overoxidation.

The permselectivity of overoxidized polyaniline towards anions was studied, and it was found that its permselectivity towards anions is driven primarily by incorporating counter anions, rather than forming new functional groups during the overoxidation process. Platinum (Pt) wire was used as the counter electrode (CE), and a saturated calomel electrode (SCE) served as the reference electrode (RE). The electrolyte was sodium chloride (KCl), and the working electrode (WE) was glassy carbon covered with PANI [9]. The electrolyte acts as a medium for electron transfer between the electrode and the analyte. In this study, PANI-SPE films were prepared via solvent casting using PANI, PVDF, LiTFSI, and PEO. Unlike prior work, the focus is on how overoxidation affects their morphological, structural, and electrochemical properties. Films with 1, 3, and 5 wt.% PANI were tested, with overoxidation induced by CV to assess its impact on conductivity and stability. The findings provide insight into degradation mechanisms and suggest strategies to improve the performance and durability of PANI-SPEs for electrochemical applications.

2. MATERIALS AND METHODS

2.1 Materials

Polyaniline (emeraldine salt) (PANI, molecular weight (Mw) ≈ 15,000 g/mol), polyethylene oxide (PEO, Mw ≈ 400,000 g/mol), polyvinylidene fluoride (PVDF, Mw ≈ 534,000 g/mol), lithium bis(trifluoromethanesulfonyl)imide (LiTFSI, ≥ 99 %) and N,N-Dimethylformamide (DMF, ≥ 99 %) were acquired from Sigma-Aldrich.

2.2 Formation of PANI-SPE Film

PANI-SPE films were prepared using the solution casting method. The base composition of PEO:PVDF:LiTFSI was fixed at a weight ratio of 7:3:2 (wt/wt/wt) [10]. PANI was incorporated as a modifier at 1 wt.% (P1), 3 wt.% (P3), and 5 wt.% (P5) relative to the total composite mass. PEO powder was first dissolved in DMF solvent under stirring, followed by the addition of PVDF powder. After two hours of stirring, LiTFSI powder was introduced into the mixture. Subsequently, PANI powder was added after another two hours of stirring. The resulting homogeneous solution was poured into a petri dish and dried in a vacuum oven at 60 °C for 24 hours, yielding uniform films with a thickness of approximately 0.02 cm.

2.3 Overoxidation of the PANI-SPE Film

Electrochemical degradation of the films through overoxidation was performed by CV using a potentiostat (Metrohm Autolab PGSTAT302N). A platinum (Pt) sheet served as the CE, the PANI-SPE film as the WE, and silver/silver chloride (Ag/AgCl) was consistently used as the RE for all measurements. The electrolyte was 0.1 M degassed KCl. To induce overoxidation, the films were cycled within the potential range of 0-1 V vs. Ag/AgCl for 10 cycles at a scan rate of 50 mV/s [9]. The laboratory setup for the films' overoxidation is displayed in Figure 1. The associated cyclic voltammograms are displayed in Figure 2. As the number of cycles increases up to 10 cycles, the current decreases, indicating a reduction in the electroactivity [3]. OP1, OP3, and OP5 are the labels assigned to the overoxidized P1, P3, and P5 films, respectively.

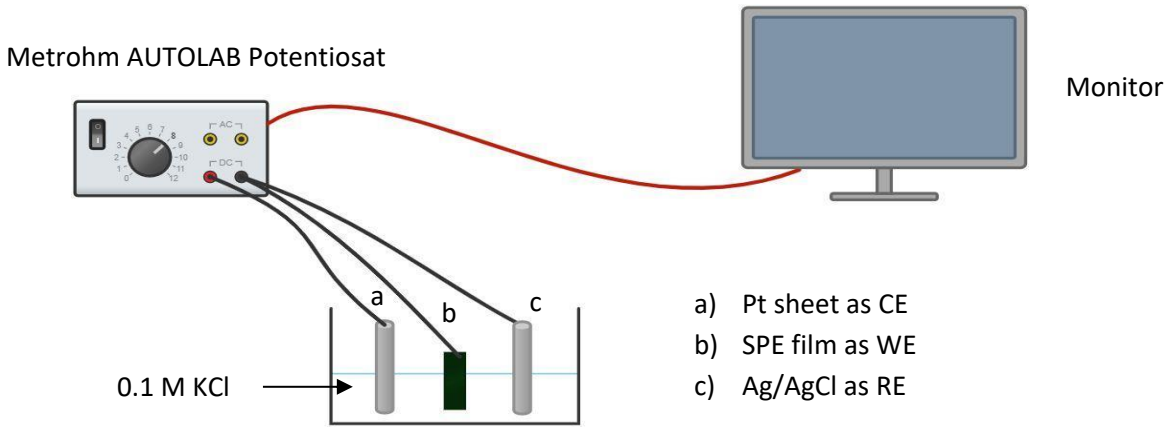

Figure 1: SPE film overoxidation experimental setup with a Pt sheet serving as the CE, PANI-SPE film as the WE, and Ag/AgCl as the RE. Overoxidation was performed using CV. 0.1 M degassed KCl was utilized as the electrolyte. For ten cycles, the SPEs were cycled between 0 and 1 V with a scan rate of 50 mV/s.

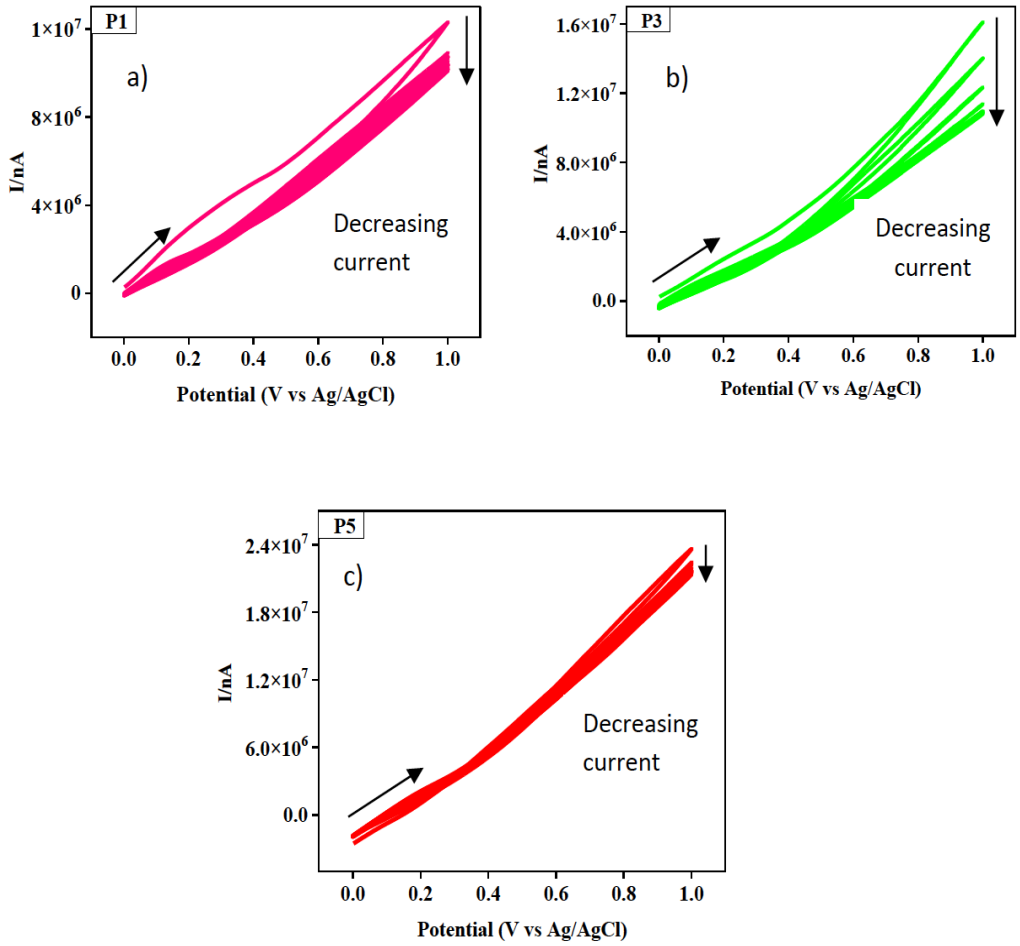

Figure 2: Cyclic voltammograms of the films (a) P1, (b) P3, and (c) P5, with a Pt sheet as the CE, Ag/AgCl as the RE, and PANI-SPE films as the WE. The scans were conducted between 0-1 V for 10 cycles at a rate of 50 mV/s.

2.4 Sample Characterization

The Shimadzu IR Affinity-1 instrument's FTIR technology was utilized to evaluate the samples' chemical makeup, with 16 scans recorded at a resolution of 4 cm^{-1}. The functional groups of all samples were examined using the American Society for Testing and Materials (ASTM) E1252 technique to determine their chemical composition. A FESEM, Carl Zeiss Supra 40VP, Germany, was used to examine the surface features of the samples. A 0.5 cm × 0.5 cm square-shaped section of the film was placed on an aluminum stub secured with double-sided carbon tape. Gold was sputter-coated onto the samples to improve the conductivity of the sample's surface. The stubs were then loaded into FESEM. High vacuum mode and 10.0 kV electron high tension (EHT) were used to record FESEM pictures. The HIOKI 3532-50 LCR Hi-TESTER PGZ100 electrochemical impedance spectroscopy (EIS) was employed to measure the conductivity of the PANI-SPE film. At room temperature, the measurements were conducted over a frequency range of 42 Hz to 5 MHz with an applied AC voltage amplitude of 10 mV RMS. Utilizing a micrometre screw gauge (Helios, 0-25 mm, 0.01 mm precision), the thickness of the membranes was determined. Two stainless steel disc electrodes with a diameter of 1 cm were sandwiched by a PANI-SPE film. EIS determines the impedance of a sample by applying a small sinusoidal or time-varying potential and measuring the resulting current response. Impedance values are recorded for various operating frequencies. The conductivity values are derived from the impedance measurements.

3. RESULTS AND DISCUSSION

3.1 Structural Properties

Figure 3 shows the chemical composition of PANI, PEO, PVDF, and LiTFSI. PANI's backbone consists of alternating benzene rings and nitrogen atoms. PANI consists of benzenoid and quinonoid rings in its structure; a benzenoid ring refers to a type of organic compound that has at least one benzene ring in its structure, while a quinonoid ring contains a six-membered carbon ring with two conjugated double bonds in the ring. PEO contains ether oxygen, which is going to help the movement of Li-ions throughout the polymer chains [2]. PVDF is a semicrystalline polymer consisting of repeating vinylidene fluoride units. The strong C-F bonds give PVDF excellent chemical resistance, thermal stability, and mechanical properties. LiTFSI has a large, asymmetric anion $(CF_3SO_2)_2N^-$ that stabilizes the lithium cations and enhances ionic mobility.

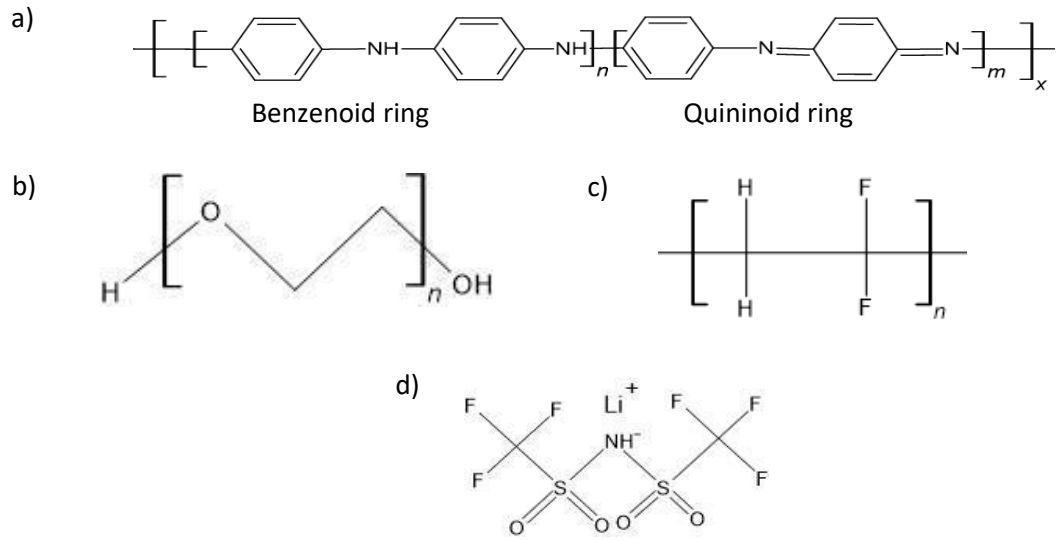

Figure 3: Chemical composition of a) PANI, b) PEO, c) PVDF, and d) LiTFSI

Figure 4 shows the FTIR spectra of the individual PANI, PEO, PVDF, and LiTFSI, which can serve as reference materials for comparison. The PANI and LiTFSI samples were in powder form, as they do not readily form standalone films. The PEO, PVDF, and composite films were analyzed in film form. It is plausible to compare the powder and film forms as the chemical structure remains consistent across forms, and the spectral features are comparable despite differences in morphology. It also displays the FTIR spectra for the films composed of varying PANI weight percentages at 1 wt.%, 3 wt.%, and 5 wt.%.

The spectrum retrieved from the LiTFSI compound presented in Figure 4(a) shows peaks at 1,634, 1,330, 1,191, 1,120, 1,048, 799, and 738 cm^{-1}, corresponding to its functional groups, according to Figure 4 [11]. Meanwhile, the spectrum that was captured on PVDF thin films displays peaks at 1,401, 1,219, 1,164, and 871 cm^{-1} [12]. PEO characteristic peaks appear at 2,879, 1,463, 1,342, 1,269, 1,092, 959, and 832 cm^{-1} [13]. In contrast, peaks related to PANI can be observed at 3,592, 1,579, 1,484, 1,302, 1,136, and 821 cm^{-1}. Figure 4 (b) shows that as the concentration of PANI increases, the spectrum at 3,592 cm^{-1}, linked to the nitrogen-hydrogen (N-H) bonding in PANI, becomes increasingly pronounced, indicating that N-H bonding in PANI intensifies with a higher amount of PANI within the composites. The carbon-hydrogen (C-H) bonding of PEO at 2,879 cm^{-1} becomes narrower and sharper as the PANI concentration increases, indicating a potential interaction between PANI and PEO.

Additionally, with higher PANI concentration, the PEO spectra corresponding to C-H bonding (2,879 cm^{-1}), oxygen-hydrogen (O-H) bonding (1,286 cm^{-1}), C-O-C bonding (1,098 cm^{-1}), CH_2 rocking motion (960 cm^{-1}), and CH_2 wagging mode (838 cm^{-1}) become narrower and sharper, further supporting the possibility of an interaction between PANI and PEO.

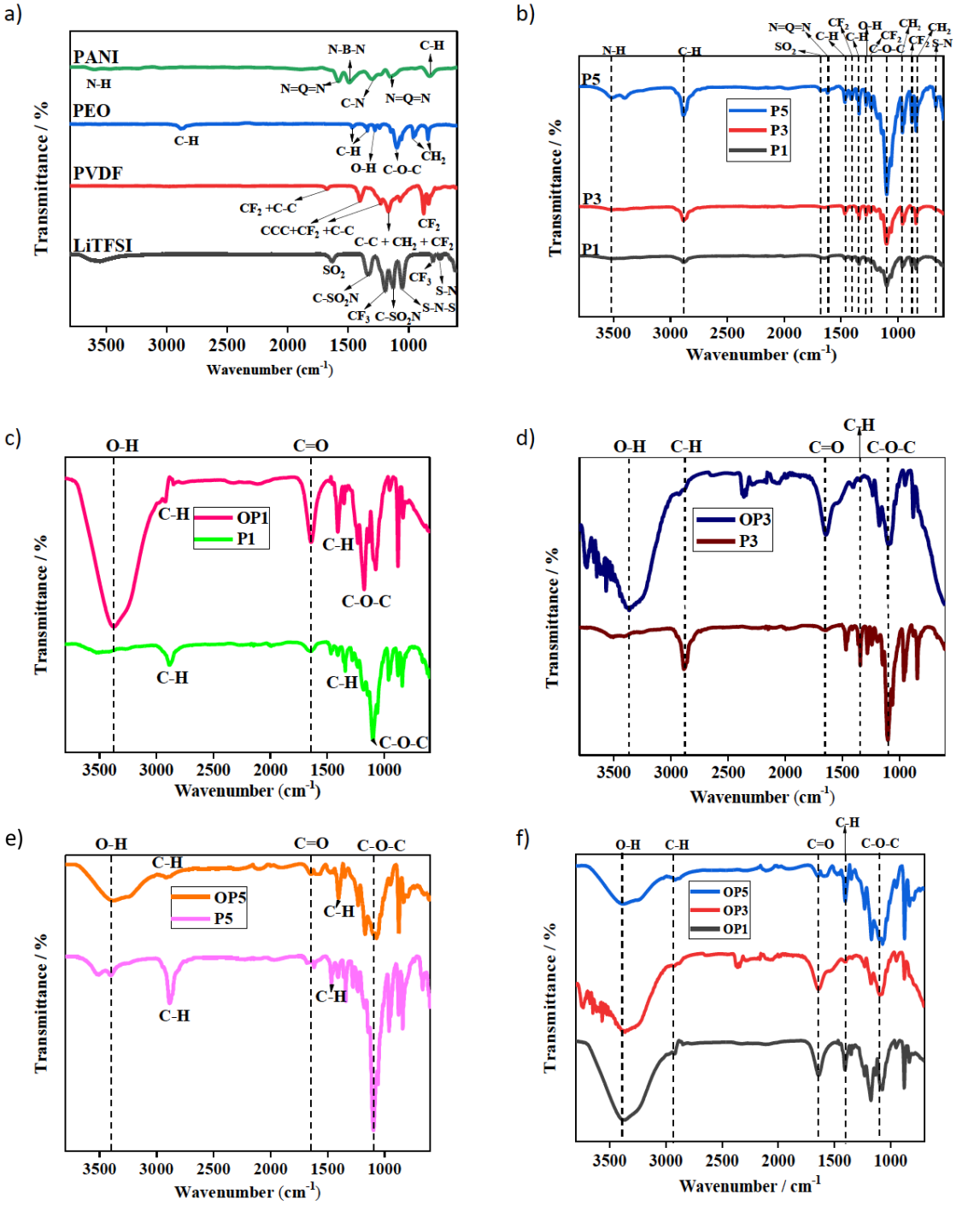

Figure 4: FTIR spectra of (a) individual PANI, PEO, PVDF, and LiTFSI of the highest purity (b) P1 film, P3 film, and P5 film (c) P1 and OP1 films (d) P3 and OP3 films (e) P5 and OP5 films (f) OP1, OP3, and OP5 films. The analysis was conducted for 16 scans with a resolution of 4 cm^{-1}, covering the spectrum of wavenumbers from 4000 cm^{-1} to 500 cm^{-1}.

After overoxidation, a new broad peak emerges at around 3,300 cm^{-1}, suggesting the formation of O-H stretching. O-H stretching indicates the formation of hydroquinone, which appeared due to the overoxidation process. The peak around 1,600 cm^{-1} becomes increasingly prominent after excessive oxidation, suggesting the formation of the C=O group of benzoquinones [8]. Of all samples upon overoxidation, the intensity of the O-H spectrum at ~3,300 cm^{-1} and the C=O spectrum at ~1,600 cm^{-1} decreases as the concentration of PANI increases. This indicates a reduction in quinone compound formation, which concludes that overoxidation declines as the concentration of PANI increases. FTIR is an effective technique for examining changes in molecular structure, bonding, and composition. It can also reveal any complexation occurring in either the amorphous or crystalline phase through the infrared spectrum.

3.2 Morphological Properties

To better comprehend how PANI concentration and excessive oxidation affect the composite, the surface characteristics of the films were investigated using FESEM. Figure 5 shows images of the PEO film, PVDF film, and composite films containing PANI, PEO, PVDF, and LiTFSI with different PANI concentrations (1 wt.%, 3 wt.%, and 5 wt.%) before and following intensive oxidation, as shown in Figure 5. The micrographs of the PEO and PVDF films are displayed in Figures 5(a) and 5(b), respectively.

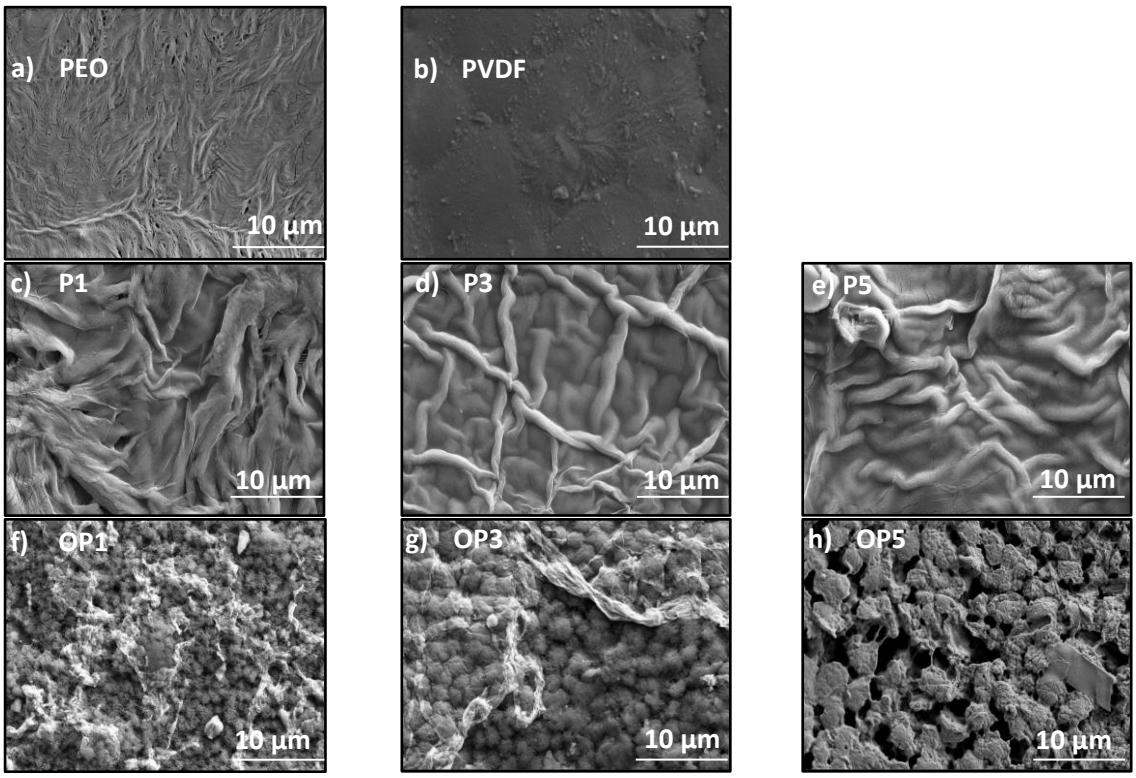

Figure 5: FESEM images of (a) PEO film, (b) PVDF film, (c) P1 film, (d) P3 film, (e) P5 film, (f) OP1 film, (g) OP3 film, and (h) OP5 film, taken at a magnification of 10,000× using the Everhart-Thornley detector (ETD) in high vacuum mode.

PEO exhibits a rigid and rough structure, as depicted in Figure 5(a), highlighting its crystalline nature. Figure 5(b) shows that the FESEM micrograph of PVDF film viewed at a magnification of 10,000× shows that the film appears to have a uniform surface with no visible cracks or tears. No significant pores are visible, indicating a dense structure. The figure also shows a significant presence of specks distributed across the surface. They are closely packed but lack a distinct pattern in their arrangement. The films of PANI:PEO:PVDF:LiTFSI display the presence of an IPN where two or more polymer networks are interlaced on a molecular scale, physically entangled in such a way that they

cannot be separated without breaking chemical bonds, although the networks are not covalently bonded to each other. The presence of an IPN can enhance the ionic conductivity of the conductive membrane [4]. FESEM images, as shown in Figure 5(c)-(e), revealed a porous structure in the P1 film, while the P3 and P5 films exhibited dense structures. It is expected that increasing the PANI concentration will lead to an increased density of the network. FESEM images showed a porous network in the P1 film, while the P3 and P5 films displayed non-porous structures. Increasing the PANI concentration is anticipated to cause densification of the network, resulting in tighter interchain packing within the polymer matrix. Excessive oxidation leads to a significant disruption in the IPN structure, characterized by the increasing number of pores and the formation of cracks, shown in Figures 5(f)-(h).

3.3 Conductivity Properties

The conductivity of PEO, PVDF, and PANI-based SPE films, prepared using the solvent casting method, was analyzed through EIS. Conductivity measurements were taken for PANI-SPE films both before and after undergoing overoxidation, allowing for a comparative analysis of the changes induced by the process. Figure 6 shows the conductivity of the PEO, PVDF, PANIS-SPE (P1, P3, P5), and overoxidized PANI-SPE (OP1, OP3, OP5) films.

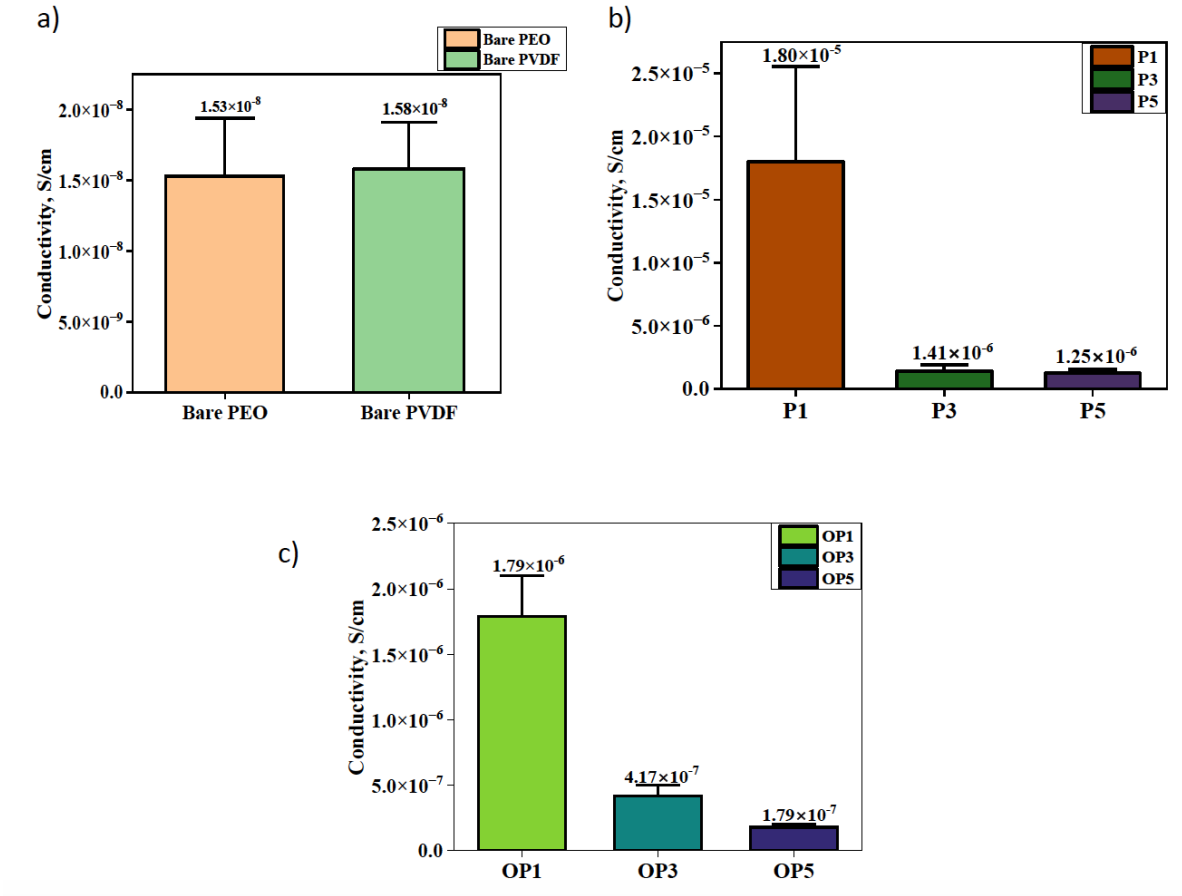

Figure 6: Conductivity values of (a) PEO and PVDF films, (b) P1, P3, and P5 films, (c) OP1, OP3, and OP5 films

Figure 6(a) shows the conductivity of the bare PEO and PVDF films, while Figures 6(b) and 6(c) display the conductivity of the P1, P3, and P5 films and the OP1, OP3, and OP5 films, respectively. The conductivity of the PEO film is 1.53×10^{-8} S/cm, in line with the reported value of PEO's conductivity, which is approximately 10^{-8} S/cm at ambient temperature [14]. The measured conductivity

of PVDF was 1.58×10^{-8} S/cm, which is notably higher than the commonly reported range of 10^{-11} S/cm to 10^{-10} S/cm [15]. Integrating a secondary polymer into a composite film enhances conductivity when compared to individual PEO and PVDF films. Figure 6(b) shows that the P1, P3, and P5 films display the mean conductivity values of 1.8×10^{-5}, 1.41×10^{-6}, and 1.25×10^{-6} S/cm, respectively. The results indicate that the conductivity decreases as the PANI concentration increases. 1 wt.% of PANI composite displayed the maximum conductivity value of 1.80×10^{-5} S/cm. Therefore, a small quantity of PANI is sufficient to improve the conductivity of the composite. This might be due to the abundance of pores in the composite with 1 wt. % of PANI, as shown in Figure 5(c). A higher porosity can improve the conductivity by offering a larger surface area for ion transport [16].

Figure 6(c) shows that after intensive oxidation, a significant decrease in conductivity is observed, as the material loses its ability to undergo electroactivity during the process. Oxidative degradation led to substantial changes in the molecular structure and physical properties of the CP [6]. As hydroxyl and carbonyl species form during oxidation at positive potentials, the electrical conductivity of the CP is reduced [17]. To provide a clearer comparison of the electrical, structural, and chemical changes observed in the composites, a summary of the key parameters before and after overoxidation is presented in Table 1. The table highlights the effect of PANI concentration on initial conductivity, the drastic reduction in conductivity after overoxidation, as well as the associated FTIR and FESEM observations.

Table 1: Summary of conductivity, FTIR, and FESEM observations of PANI-based SPE composites before and after overoxidation

Samples	PANI wt.%	Initial Conductivity (S/cm)	Final Conductivity (S/cm)	% Decrease	Changes in chemical structure	Changes in morphology
P1	1	1.80×10^{-5}	1.79×10^{-6}	90.1 %	O-H, C=O formed	Porous → cracks/pores
P3	3	1.41×10^{-6}	4.17×10^{-7}	70.4 %	O-H, C=O formed	Dense → cracks
P5	5	1.25×10^{-6}	$1.79X10^{-7}$	85.7 %	O-H, C=O formed	Dense → cracks/rupture

4. CONCLUSIONS

This study examined the effects of overoxidation on PANI-based SPE composites for LIBs, focusing on structural, electrical, and morphological changes. The conductivity decreased significantly from 1.80×10^{-5} S/cm (1 wt.% PANI composite) to values near 10^{-8} S/cm after overoxidation, indicating severe loss of electroactivity. Structurally, FESEM revealed increased pores, cracks, and reduced film thickness, confirming degradation of the IPN network, while FTIR verified the formation of hydroxyl and carbonyl groups as oxidation products. These results emphasize the detrimental impact of overoxidation and the need for mitigation strategies to maintain composite performance in LIB applications.

Acknowledgements

The authors gratefully acknowledge PETRONAS Research Sdn. Bhd. for funding support, as well as the Faculty of Applied Sciences, Universiti Teknologi MARA (UiTM) Shah Alam, for providing

research facilities. This work was also financially supported by UiTM and the Institute of Postgraduate Studies, UiTM.

Author Contributions

All authors contributed to data analysis, drafting, and critically revising the paper and agree to be accountable for all aspects of the work.

Disclosure of Conflict of Interest

The authors declare no disclosures.

Compliance with Ethical Standards

The work is compliant with ethical standards.

References

[1] Murata, K., Izuchi, S. & Yoshihisa, Y. (2000). An overview of the research and development of solid polymer electrolyte batteries. *Electrochimica Acta*. *45(8–9)*, 1501–1508.

[2] Chen, H., Zheng, M., Qian, S., Ling, H. Y., Wu, Z., Liu, X., Yan, C. & Zhang, S. (2021). Functional additives for solid polymer electrolytes in flexible and high-energy-density solid-state lithium-ion batteries. *Carbon Energy*. *3(6)*, 929–956.

[3] Leš, K. & Jordan, C. (2020). Ionic conductivity enhancement in solid polymer electrolytes by electrochemical in situ formation of an interpenetrating network. *RSC Advances. 10(68)*, 41296.

[4] Tan, S., Zeng, X., Ma, Q., Wu, X. & Guo, Y. (2018). Recent advancements in polymer-based composite electrolytes for rechargeable lithium batteries. *Electrochemical Energy Reviews*. *1(2)*, 113–138.

[5] Fong, K. D., Wang, T., Kim, H., Kumar, R.V. & Smoukov, S.K. (2017). Semi-interpenetrating polymer networks for enhanced supercapacitor electrodes. *ACS Energy Letters*. *2(9)*, 2014–2020.

[6] Holze, R. (2022). Overoxidation of intrinsically conducting polymers. *Polymers*. *14(8)*, 1584.

[7] Beygisangchin, M., Rashid, S. A., Shafie, S., Sadrolhosseini, A. R. & Lim, H. N. (2021). Preparations, properties, and applications of polyaniline and polyaniline thin films-A review. *Polymers*. *13(12)*, 2003.

[8] Gao, M., Zhang, G., Zhang, G., Wang, X., Wang, S. & Yang, Y. (2011). The resistance to over-oxidation for polyaniline initiated by the resulting quinone-like molecules. *Polymer Degradation and Stability*. *96(10)*, 1799–1804.

[9] Mondal, S. & Sangaranarayanan, M. V. (2016). Permselectivity and thickness-dependent ion transport properties of overoxidized polyaniline: a mechanistic investigation. *Physical Chemistry Chemical Physics. 18(44)*, 30705–30720.

[10] Li, J., Zhu, K., Wang, J., Yan, K., Liu, J., Yao, Z. & Xu, Y. (2020). Optimisation of conductivity of PEO/PVDF-based solid polymer electrolytes in all-solid-state Li-ion batteries. *Materials Technology*, *37(4)*, 240–247.

[11] Kam, W., Liew, C., Lim, J. Y. & Ramesh, S. (2013). Electrical, structural, and thermal studies of antimony trioxide-doped poly(acrylic acid)-based composite polymer electrolytes. *Ionics*. *20(5)*, 665–674.

[12] Sousa, E. A., Deniz, W. D. S., Arlindo, E. P. S., Sakamoto, W. K. & Fuzari, G. C. (2016). PVDF-PAni blend: a free-standing film with variable electrical resistance. *Polymer Bulletin*. *74(5)*, 1483–1492.

[13] Morsi, M. A., Abdelrazek, E. M. & Abdelghany, A. M. (2016). Evaluation of optical parameters and structural variations of UV irradiated (PEO/PVP)/Au polymer nanocomposites. *Research Journal of Pharmaceutical, Biological and Chemical Sciences*. *7(2)*, 1877–1890.

[14] Gucci, F., Grasso, M., Russo, S., Leighton, G.J.T., Shaw, C. & Brighton, J. (2023). Electrical and mechanical characterisation of poly(ethylene)oxide-polysulfone blend for composite structural lithium batteries. *Polymers*. *15(11)*, 2581.

[15] Salam, M. A., Elkomy, G., Osman, H., Nagy, M. & El-Sayed, F. (2012). Structure–electrical conductivity of polyvinylidene fluoride/graphite composites. *Journal of Reinforced Plastics and Composites*. *31(20)*, 1342–1352.

[16] Beuse, T., Fingerle, M., Wagner, C., Winter, M. & Börner, M. (2021). Comprehensive insights into the porosity of lithium-ion battery electrodes: a comparative study on positive electrodes based on $LiNi_{0.6}Mn_{0.2}Co_{0.2}O_2$ (NMC622). *Batteries*. *7(4)*, 70.

[17] Rodríguez, I., Scharifker, B. & Mostany, J. (2000). In situ FTIR study of redox and overoxidation processes in polypyrrole films. *Journal of Electroanalytical Chemistry*. *491(1–2)*, 117–125.